Twinfilin is an actin-filament-severing protein and promotes rapid turnover of actin structures in vivo

James B. Moseley[1], Kyoko Okada[1], Heath I. Balcer[1], David R. Kovar[2], Thomas D. Pollard[2] and Bruce L. Goode[1,*]

[1]Department of Biology and The Rosenstiel Basic Medical Sciences Research Center, Brandeis University, Waltham, MA 02454, USA
[2]Department of Molecular, Cellular and Developmental Biology, Yale University, New Haven, CT 06520, USA
*Author for correspondence (e-mail: goode@brandeis.edu)

Accepted 28 December 2005
Journal of Cell Science 119, 1547-1557 Published by The Company of Biologists 2006
doi:10.1242/jcs.02860

Summary

Working in concert, multiple actin-binding proteins regulate the dynamic turnover of actin networks. Here, we define a novel function for the conserved actin-binding protein twinfilin, which until now was thought to function primarily as a monomer-sequestering protein. We show that purified budding yeast twinfilin (Twf1) binds to and severs actin filaments in vitro at pH below 6.0 in bulk kinetic and fluorescence microscopy assays. Further, we use total internal reflection fluorescence (TIRF) microscopy to demonstrate that Twf1 severs individual actin filaments in real time. It has been shown that capping protein directly binds to Twf1 and is required for Twf1 localization to cortical actin patches in vivo. We demonstrate that capping protein directly inhibits the severing activity of Twf1, the first biochemical function ascribed to this interaction. In addition, phosphatidylinositol (4,5)-bisphosphate [PtdIns(4,5)P_2] inhibits Twf1 filament-severing activity. Consistent with these biochemical activities, a *twf1*Δ mutation causes reduced rates of cortical actin patch turnover in living cells. Together, our data suggest that twinfilin coordinates filament severing and monomer sequestering at sites of rapid actin turnover and is controlled by multiple regulatory inputs.

Supplementary material available online at
http://jcs.biologists.org/cgi/content/full/119/8/1547/DC1

Key words: Actin, Yeast, Twinfilin, Capping protein, Cofilin

Introduction

Dynamic actin filament networks facilitate a multitude of cellular functions, including cell motility, endocytosis, polarized vesicle secretion and cell division. The coordinated activities of multiple actin-binding proteins regulate such networks by controlling the assembly, stability and subsequent disassembly of actin filaments. To date ADF/cofilin proteins are the only widely conserved factors shown to promote actin dynamics by severing filaments and/or promoting subunit dissociation (Theriot, 1997; Bamburg, 1999; Carlier et al., 1999). In the budding yeast *Saccharomyces cerevisiae*, cofilin (*COF1*) is an essential gene (Iida et al., 1993; Moon et al., 1993), and mutations (such as *cof1-22*) that impair filament severing and/or depolymerization in vitro have severe growth and actin turnover defects in vivo (Lappalainen and Drubin, 1997; Lappalainen et al., 1997). A second factor implicated in yeast actin turnover is the highly conserved actin-binding protein twinfilin (Twf1). In all species examined, twinfilin localizes to sites of rapid actin turnover, such as cortical actin patches in yeast (Goode et al., 1998) and filopodia in mammalian cells (Vartiainen et al., 2000; Vartiainen et al., 2003). In *twf1*Δ yeast cells, the actin cytoskeleton is only mildly perturbed, with increased actin staining at cortical patches (Goode et al., 1998). However, deletion of *TWF1* is synthetically lethal with the *cof1-22* mutation. This has raised the possibility that twinfilin helps promote actin turnover; however, direct evidence for such a function has been lacking.

Twinfilin comprises tandem ADFH (for 'actin depolymerizing factor/cofilin homology') domains connected by a short linker (Goode et al., 1998; Lappalainen et al., 1998; Palmgren et al., 2002). The crystal structure of one ADFH domain from twinfilin reveals a fold very similar to ADF/cofilins (Paavilainen et al., 2002). However, unlike cofilin, twinfilin binds tightly to and sequesters actin monomers [K_d~0.5 μM for ATP-actin, 0.05 μM for ADP-actin (Ojala et al., 2002)], with no reported affinity for actin filaments (Goode et al., 1998; Vartiainen et al., 2000; Wahlstrom et al., 2001; Ojala et al., 2002; Vartiainen et al., 2003). Whereas ADF/cofilin binds to actin filaments in multiple in vitro assays, including actin filament disassembly reactions, twinfilin has no apparent effects in such assays (Goode et al., 1998; Vartiainen et al., 2000). Thus, Twf1 has been proposed to function exclusively as an actin-monomer-sequestering protein (reviewed by Palmgren et al., 2002).

Twinfilin also associates with capping protein, as demonstrated by co-immunoprecipitation from cell extracts, colocalization in vivo and direct binding using purified proteins (Palmgren et al., 2001; Falck et al., 2004). Capping protein is required for the proper localization of Twf1 in yeast cells (Palmgren et al., 2001; Kovar et al., 2005), and the structure of the twinfilin-capping protein complex has been solved using X-ray scattering (Falck et al., 2004). However, capping protein has no detectable effects on the ability of twinfilin to sequester actin monomers and, reciprocally, twinfilin has no detectable

effects on the ability of capping protein to cap filament ends. Thus, no function has yet been ascribed to this physiological interaction.

Phosphorylation and pH regulate the actin-filament-severing and/or actin-depolymerization activities of many ADF/cofilins (Bamburg, 1999). *S. cerevisiae* Cof1 does not appear to be phosphorylated (Lappalainen et al., 1997), but is reported to display some pH dependence of its activities (Iida et al., 1993; Du and Frieden, 1998). Given that Twf1 comprises two ADFH domains, we examined its ability to interact with actin filaments across a broad range of pH values. We found that Twf1 interacts with actin filaments and promotes filament severing in a pH-dependent manner. Furthermore, the yeast heterodimeric capping protein (CP) directly inhibits Twf1 binding to and severing of actin filaments, but not Twf1 interactions with monomers. Deletion of the *TWF1* gene reduces rates of actin filament turnover at cortical patches. This provides in vivo support for the biochemical activities described above, and represents the first demonstration in any species that twinfilin promotes actin turnover. Taken together, these results provide a new mechanism for Twf1 function in regulating actin dynamics and shed light on the previously enigmatic CP-Twf1 interaction.

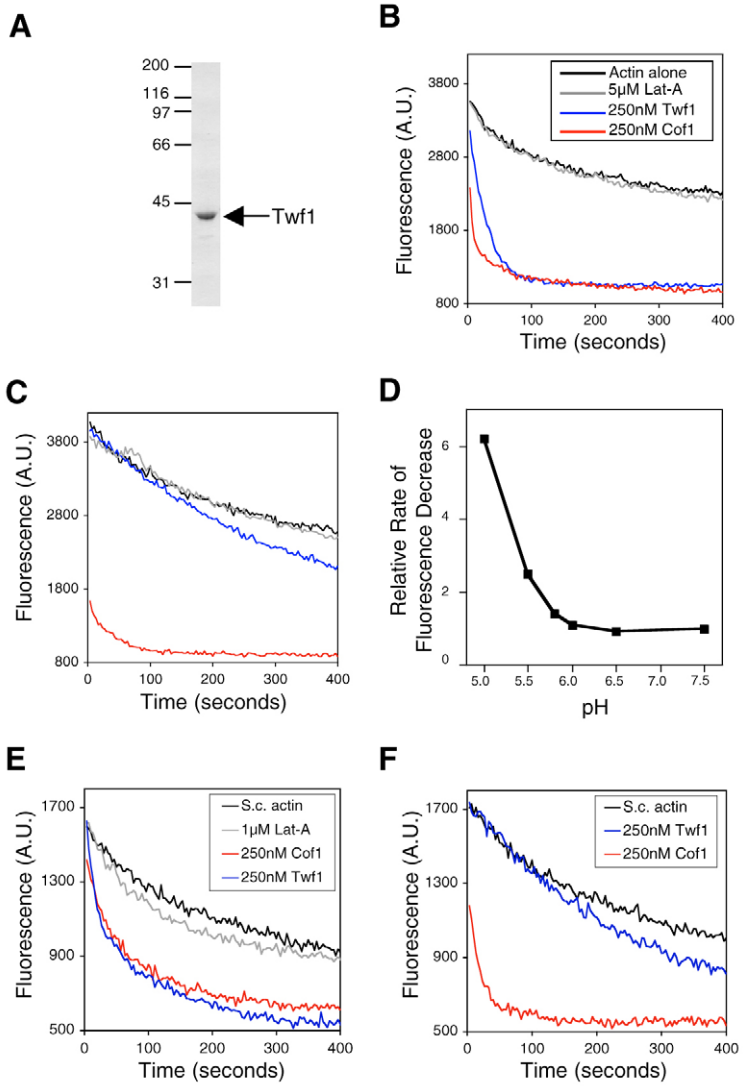

Fig. 1. *S. cerevisiae* twinfilin (Twf1) binds to and depolymerizes actin filaments in a pH-dependent manner. (A) Coomassie-stained SDS-polyacrylamide gel of purified Twf1. Positions of molecular mass markers (kDa) are indicated. (B,C) Time course of actin filament fluorescence (rabbit skeletal muscle actin; 30% pyrene labeled) after dilution at time zero (from 5 μM to 0.1 μM) alone or in the presence of Cof1, Twf1 or Lat-A at pH 5.0 (B) or pH 5.8 (C). The inset legend for B also applies to C. (D) Initial rate of actin filament fluorescence decrease induced by 250 nM Twf1 (reaction conditions as in B,C) as a function of pH in the reaction. The rate of fluorescence decrease for actin alone was set at 1 to reference Twf1 effects. (E,F) Time course of actin filament fluorescence (*S. cerevisiae* actin; 30% pyrene labeled) after dilution at time zero (from 5 μM to 0.1 μM) alone or in the presence of Cof1, Twf1 or Lat-A at pH 5.0 (E) or pH 7.5 (F).

Results

Previously, budding yeast Twf1 was tested for filament binding only at pH 7.5 (Goode et al., 1998), so we examined the effects of Twf1 on actin filaments over a pH range. Pyrene-labeled actin filaments were diluted from 5 μM to the critical concentration of 0.1 μM to induce net disassembly in the presence and absence of other purified proteins. The loss of pyrene fluorescence signal in this assay is proportional to the rate of filament disassembly. Therefore, actin monomer sequestering [e.g. see latrunculin-A (Lat-A) effects below] does not significantly affect the rate of filament disassembly in this assay; only factors that bind to filaments strongly affect the fluorescence kinetics. Factors that sever and/or accelerate subunit dissociation from filament ends can induce rapid disassembly to accelerate loss of fluorescence. In addition, some proteins quench the fluorescence of pyrene-labeled actin filaments upon binding, as reported for cofilin (Moon et al., 1993; Carlier et al., 1997; Blanchoin and Pollard, 1999).

The addition of Twf1 to pyrene-labeled actin filaments at pH 5.0 and pH 5.5 induced an exponential decrease in fluorescence, with kinetics similar to reactions containing an equivalent concentration of Cof1 (Fig. 1B and data not shown). However, Twf1 did not change the fluorescence at or above pH 6.0 (Fig. 1D), whereas Cof1 maintained its effects at higher pH values (Fig. 1C and data not shown). This pH-dependent effect was observed using either rabbit skeletal muscle (Fig. 1B,C) or *S. cerevisiae* pyrene-labeled actin filaments (Fig. 1E,F). At pH lower than 6.0, Twf1 decreased fluorescence levels in a concentration-dependent manner (Fig. 2A,B), with potency similar to Cof1 (Fig. 2C and data not shown). All reactions eventually reached the same baseline fluorescence (not shown), indicating that filaments completely depolymerize under these conditions. Excess Lat-A, a drug that sequesters actin monomers, did not significantly affect fluorescence kinetics at different pH values (Fig. 1B,C and data not shown). Thus, the effects of Twf1 in this assay are distinct from monomer sequestering.

ADF/cofilin quenches the fluorescence of pyrene-labeled actin filaments (Moon et al., 1993; Carlier et al., 1997; Blanchoin and Pollard, 1999), and thus its effects on the fluorescence signal might reflect binding

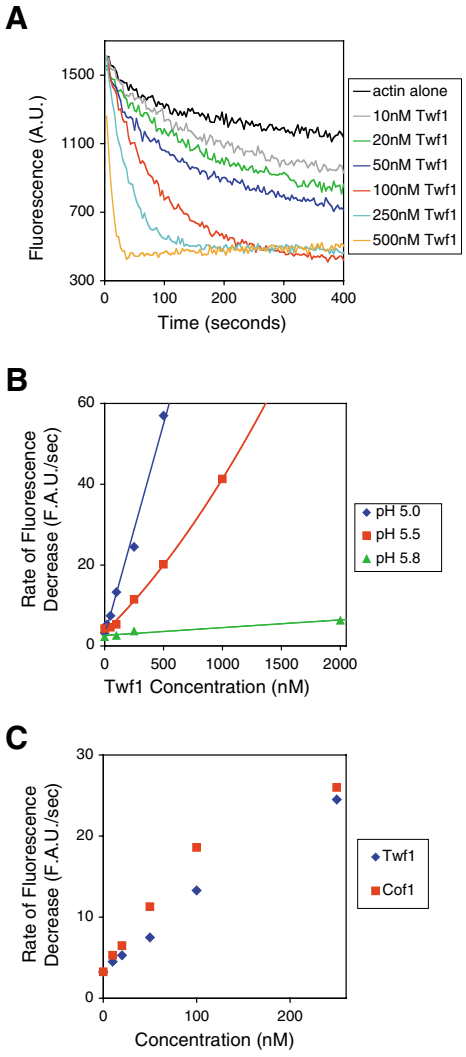

Fig. 2. Concentration-dependent effects of Twf1 on rates of dilution-induced actin filament disassembly. (A) Time course of actin filament fluorescence upon dilution (as in Fig. 1) in the presence of a range of concentrations of Twf1 at pH 5.0. (B) Concentration-dependent effects of Twf1 on the initial rate of decrease of actin filament fluorescence at different pH values. Rates were obtained from fluorescence curves in A and data not shown. (C) Comparison of Twf1 and Cof1 effects on the initial rate of actin filament fluorescence decrease at pH 5.0. Rates were obtained from fluorescence curves in A and data not shown. F.A.U., fluorescence arbitrary units.

to filaments independent of depolymerization. Given the similarities between Cof1 and Twf1 in sequence (Goode et al., 1998) and structure (Paavilainen et al., 2002), we considered that the effects of Twf1 in these assays might also reflect fluorescence quenching from binding, independent of depolymerization. Therefore, we performed two independent tests of whether Twf1 and/or Cof1 promote filament depolymerization. First, we examined filament disassembly kinetics by light scattering, and observed a similar pH-dependent acceleration of filament disassembly by Twf1 (Fig. 3A,B). By contrast, Lat-A had little effect on filament light scattering at pH 5.0 (data not shown). These results demonstrate further that Twf1 filament disassembly activity is distinct from its monomer-sequestering activity. However, we note that Twf1 and Cof1 both induced slower rates of filament disassembly monitored by light scattering than by pyrene fluorescence, suggesting that the pyrene-labeled actin disassembly assays (Figs 1 and 2) might measure Twf1 binding to actin filaments prior to its effects on disassembly.

As a second independent test, we removed aliquots from depolymerization reactions at different time points, stabilized filaments with Alexa Fluor 488-conjugated phalloidin, and imaged them by fluorescence microscopy. In reactions containing actin alone (no Cof1 or Twf1), the number and length of filaments decreased incrementally over 10 minutes of dilution-induced disassembly (Fig. 3C), consistent with the slow kinetics of pyrene-labeled actin filament disassembly (Fig. 1B). Reactions containing Lat-A appeared similar to actin-alone reactions in both the number and length of filaments (Fig. S1, supplementary material). By contrast, the addition of either Twf1 or Cof1 induced a rapid decrease in the length and number of filaments (Fig. 3C), suggesting that both Twf1 and Cof1 promote rapid filament depolymerization in these assays. In summary, Twf1 and Cof1 might quench the pyrene-labeled actin signal in depolymerization assays but, as demonstrated by two additional tests, they promote depolymerization after binding to filaments.

We considered two mechanisms by which Twf1 might promote filament disassembly: (1) severing filaments or (2) accelerating subunit dissociation from filament ends. To test these mechanisms, we examined Twf1 effects on individual actin filaments by time-lapse total internal reflection fluorescence (TIRF) microscopy. This method removes assumptions inherent to bulk kinetic assays and permits direct observation of protein activity on the dynamics of single actin filaments (Amann and Pollard, 2001; Kovar et al., 2003; Kuhn and Pollard, 2005). Fluorescently labeled actin filaments incubated in control buffer (Fig. 4A and Movie 1, supplementary material) or Lat-A (Fig. 4B and Movie 2, supplementary material) at pH 5.0 were stable for over 15 minutes. By contrast, the addition of Twf1 caused rapid severing of actin filaments along their visible lengths (Fig. 4C and Movie 3, supplementary material). Consistent with our bulk pyrene fluorescence assays, Twf1 did not induce severing in TIRF reactions at pH 7.0 (data not shown).

To determine whether severing of filaments by Twf1 generates free barbed ends, we flowed in fresh actin monomers to TIRF reactions containing Twf1-severed filaments. These severed filaments, which appeared as short fragments of F-actin, rapidly elongated upon addition of monomeric actin (Fig. 4D and Movie 3, supplementary material). We concluded that elongation occurred at free barbed ends based on two criteria: (1) prior to Twf1 severing, filament orientation was determined from the growth rates at the two ends; (2) the severed ends elongated at approximately the rates of free barbed ends (8.9 μM^{-1} $second^{-1}$; 10 filaments measured). These results suggest that Twf1 induces actin disassembly at least in part by severing filaments. Consistent with a severing mechanism, Twf1 decreased fluorescence of pyrene-labeled actin filaments capped at their barbed ends by gelsolin (Fig. 5). Adherence of actin filaments to the slides at pH 5.0 precluded measurement of the disassembly rates at filament ends by TIRF microscopy. Furthermore, Twf1 access to adhered filaments might be

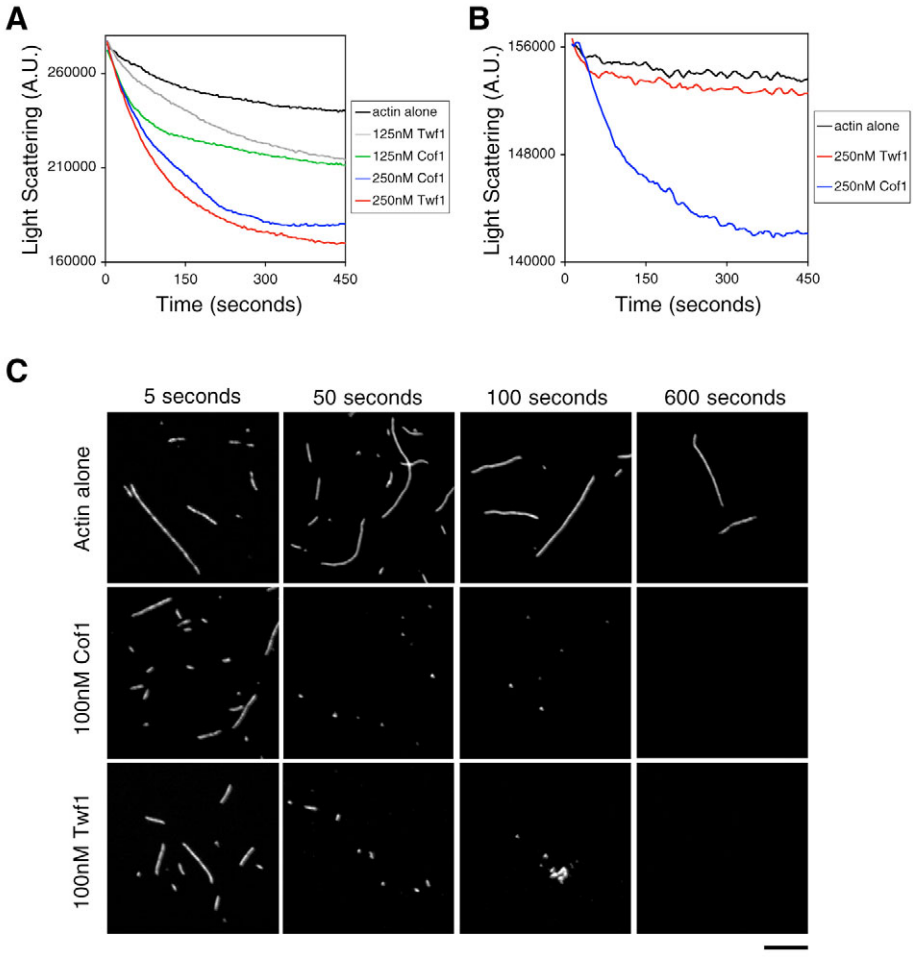

Fig. 3. Twf1 and Cof1 promote actin filament disassembly in dilution-induced assays. (A,B) Time course of unlabeled actin filament light scattering (monitored at 400 nm) after dilution at time zero, from 5 μM to 0.25 μM, in the presence of indicated proteins at pH 5.0 (A) or pH 7.5 (B). A.U., arbitrary units. (C) Fluorescence micrographs of actin filaments incubated alone or with 100 nM Cof1 or Twf1 as in Fig. 1B. At the indicated time points, samples were removed from dilution-induced reactions, incubated with Alexa Fluor 488-congugated phalloidin, and visualized by light microscopy. Bar, 5 μm.

restricted, as Twf1 severing observed by TIRF appears to be less efficient than Twf1 effects in pyrene fluorescence and light scattering reactions. Thus, our TIRF analysis might in fact underestimate the efficiency of Twf1 severing.

We next examined the effects of heterodimeric yeast capping protein CP on filament severing by Twf1. In pyrene-labeled actin disassembly reactions, CP reduced rates of filament disassembly as expected by blocking dissociation of subunits from the barbed ends of filaments (Fig. 6A). In reactions containing both CP and Twf1, CP attenuated the effects of 250 nM Twf1 in a concentration-dependent manner (Fig. 6B,C). 1 μM CP also inhibited the effects of 100 nM Twf1 on the number and length of filaments in light microscopy assays (Fig. S1, supplementary material). On the basis of the CP concentration required for 50% inhibition of Twf1 activity, we estimate an apparent K_d of 100 nM for CP binding to Twf1. From this estimation, we calculated a theoretical curve for the effects of CP on Twf1 activity (Fig. 6C). For these calculations, we first determined the concentration of free Twf1 (i.e. not bound to CP), given a K_d of 100 nM, and next calculated the effects of these Twf1 concentrations on pyrene fluorescence (based on concentration dependence curves in Fig. 2B). From this analysis, the CP-Twf1 interaction appears to be even stronger than the estimated K_{app} of 100 nM; determination of the precise affinity will require further experiments.

The observed inhibition of Twf1 filament binding and severing by CP is consistent with two potential mechanisms. First, Twf1 might be inhibited by its direct binding interaction with CP. This mechanism is supported by the observation that CP inhibits Twf1 effects in pyrene fluorescence disassembly assays, which probably measure filament binding and quenching by Twf1. Second, CP might stabilize free barbed ends generated by Twf1 severing, independent of a direct CP-Twf1 interaction. To distinguish between these two mechanisms, we visualized actin filament dynamics by TIRF microscopy in the combined presence of Twf1 and CP. Under these conditions, Twf1 induced very few severing events (Fig. 6D and Movie 4, supplementary material). Similar to our bulk kinetic data, this suggests that CP directly inhibits Twf1 binding to, and severing of, filaments. The rare severing events observed in the combined presence of Twf1 and CP did not generate free barbed ends, as demonstrated by failure of those ends to elongate upon addition of fresh actin monomers (Fig. 6E and Movie 4, supplementary material). This suggests that the new filament ends were capped. We speculate that infrequent severing events are mediated by the small subset of Twf1 molecules in the reaction that are free (i.e. not bound to CP) at any given moment. However, the new barbed ends generated by severing are capped rapidly by CP (free or complexed with Twf1). These data are consistent with previous work showing that twinfilin does not affect the capping activity of CP (Falck et al., 2004).

To test if CP inhibition of Twf1 requires their direct association, we purified a twinfilin mutant (Twf1-10) lacking

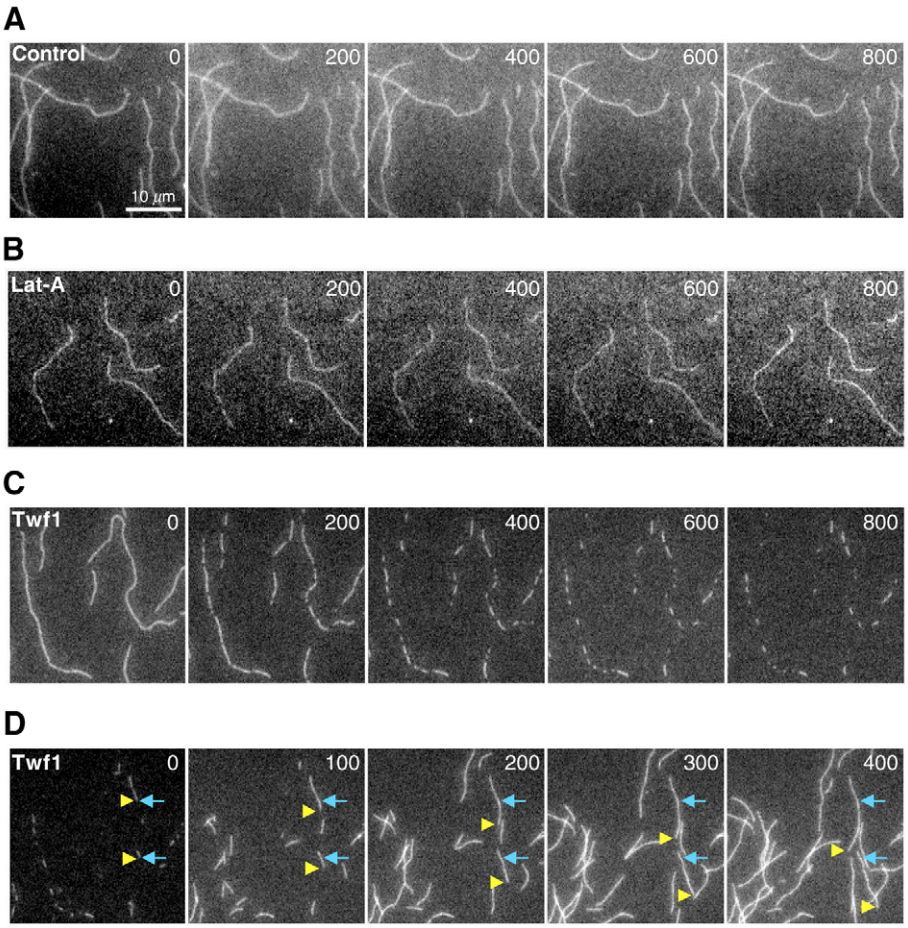

Fig. 4. Time-lapse TIRF microscopy of Twf1 severing actin filaments. (A-C) 1.5 μM monomeric actin (30% Alexa Fluor 488 labeled) was assembled into filaments in a flow cell, and then control buffer at pH 5.0 (A), 10 μM Lat-A at pH 5.0 (B), or 2 μM Twf1 at pH 5.0 (C) was applied at time zero. The time in seconds following addition of buffer/proteins is shown in the upper right corner of each panel. (D) Following filament severing by Twf1 in C, the immobilized filaments were incubated with fresh 1.5 μM actin monomers (30% Alexa Fluor 488 labeled) at time zero. Yellow arrowheads track the growth of barbed ends in consecutive frames (barbed end growth rate 8.9 μM^{-1} $second^{-1}$, 10 filaments measured). Blue arrows mark the original positions of barbed ends (at time zero) for frame of reference. The field in D is the same field as that shown in C. Movies of these TIRF microscopy experiments are provided in supplemental materials (Movies 1-3, supplementary material).

the C-terminal 10 residues (ΔP_{323}-T_{332}) that mediate CP binding (Fig. 7A). Twf1-10 does not detectably bind to CP, but maintains actin-monomer-sequestering activity (Falck et al., 2004). In pyrene-labeled actin filament disassembly reactions, Twf1-10 induced a rapid decrease in fluorescence at pH 5.0, with kinetics similar to wild-type Twf1 (Fig. 7B), indicating that Twf1-10 has a normal interaction with actin filaments. However, 1 μM CP did not significantly affect Twf1-10 activity in the assay, in contrast to its effects on wild-type Twf1 (Fig. 7B). These data strongly support a model whereby CP directly inhibits Twf1 interactions with actin filaments. The minor negative effects of 1 μM CP on reactions containing Twf1-10 probably reflect capping of barbed ends and resulting inhibition of depolymerization (similar to its activity on actin alone).

In addition, we examined the effects of CP on Twf1-10 activity by TIRF microscopy. Similar to wild-type Twf1, Twf1-10 severed filaments to generate free barbed ends that rapidly elongated upon addition of fresh actin monomers (Fig. 7C,D and Movie 5, supplementary material). However, Twf1-10 efficiently severed actin filaments in the presence of 3 μM CP (Fig. 7E and Movie 6, supplementary material), which nearly abolishes severing by wild-type Twf1 (Fig. 6D). Interestingly, the barbed ends generated by Twf1-10 severing in the presence of CP fail to elongate upon addition of fresh actin monomers (Fig. 7F and Movie 6, supplementary material), demonstrating that CP readily caps those filament ends. Taken together, our data from bulk kinetic and TIRF assays demonstrate that CP directly inhibits Twf1 binding to, and severing of, actin filaments.

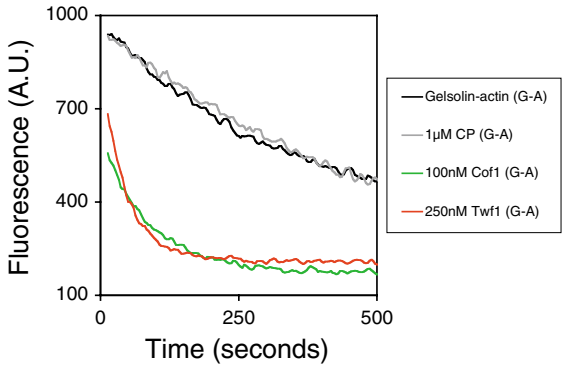

Fig. 5. Effects of Twf1 and Cof1 on the fluorescence of actin filaments capped at their barbed ends with gelsolin. Time course of gelsolin-capped actin filament (G-A) fluorescence (40% pyrene labeled) at pH 5.0 after dilution (from 5 μM to 0.25 μM) at time zero in the presence of the indicated proteins. Actin (5 μM) was polymerized in the presence of 25 nM gelsolin. 1 μM CP had no effect on the depolymerization rate, verifying that these filaments were capped efficiently at their barbed ends by gelsolin. A.U., arbitrary units.

Twf1, like Cof1, binds directly to the phospholipid phosphatidylinositol (4,5)-bisphosphate [PtdIns(4,5)P_2], which inhibits Twf1 binding to actin monomers (Palmgren et al., 2001) and Cof1 binding to actin monomers and filaments (Bamburg, 1999). In pyrene-labeled actin filament disassembly assays, the effects of Twf1 and Cof1 were fully attenuated by 20 μM PtdIns(4,5)P_2 (Fig. 8). This PtdIns(4,5)P_2 concentration is comparable with levels (50 μM) required for efficient inhibition of Twf1 monomer binding (Palmgren et al., 2001). The ability of PtdIns(4,5)P_2 to inhibit both monomer and filament binding by Twf1 is in contrast to CP, which specifically regulates Twf1 interaction with filaments but not monomers.

Although most of our assays show that Cof1 and Twf1 sever actin filaments similarly (at low pH), one key difference is that severing by Twf1, but not by Cof1, appears to be inhibited by excess actin monomers. In filament elongation reactions containing pre-formed filaments and actin monomers, Cof1 accelerated assembly, consistent with severing to increase the number of free barbed ends. By contrast, Twf1 inhibited assembly, consistent with monomer sequestering (data not shown). This effect is probably due to Twf1 binding to actin monomers with high affinity and preventing their addition to filament ends (Goode et al., 1998). To control for such effects, we added high concentrations of profilin to the filament elongation reactions. Profilin binds with high affinity to ATP-actin monomers (out-competing Twf1), and yet permits addition of monomers onto the barbed ends of filaments. In the presence of profilin at pH 5.0, Cof1 and Twf1 both stimulated actin assembly (Fig. 9), consistent with severing of the pre-formed filaments. Thus, high concentrations of profilin-actin, such as those found in cells, facilitate Twf1 severing of filaments.

Given these newly identified activities for Twf1 and the specificity of these effects occurring at lower pH, it was important to test whether Twf1 promotes actin filament disassembly in living cells grown under standard conditions. Twf1 and Cof1 both localize in yeast to cortical actin patches

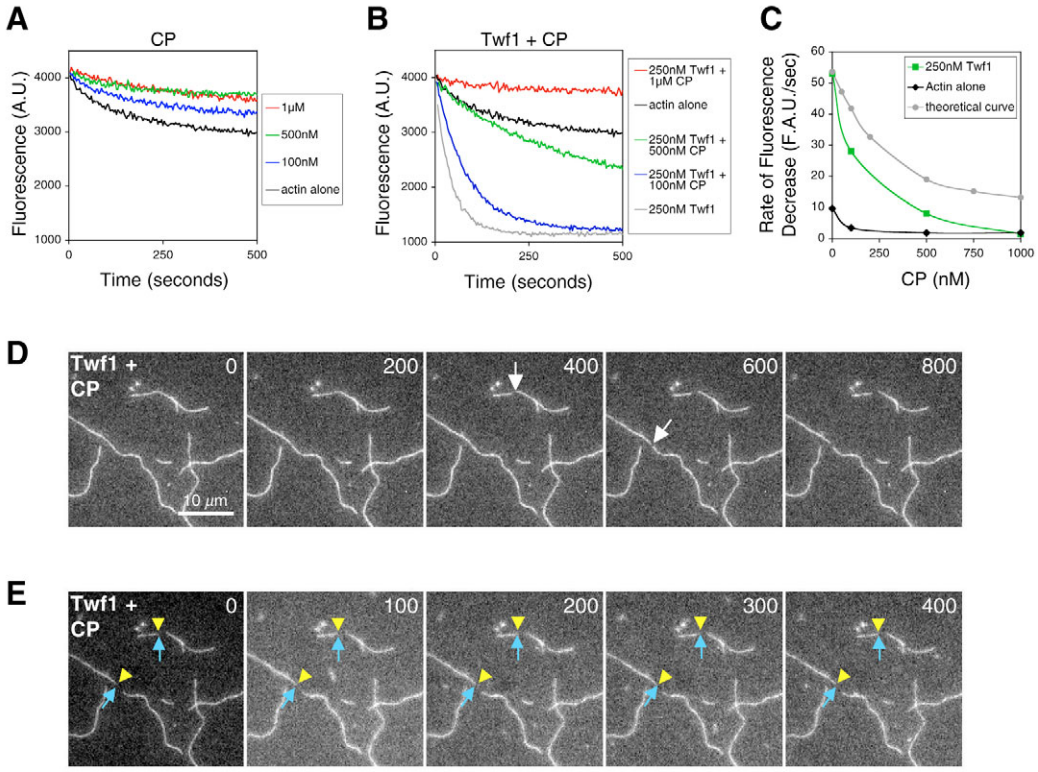

Fig. 6. *S. cerevisiae* capping protein (CP) inhibits Twf1 binding to and severing actin filaments. (A) Time course of actin filament fluorescence (40% pyrene labeled) after dilution at time zero (from 5 μM to 0.1 μM) in the presence of the indicated concentrations of CP at pH 5.0. A.U., arbitrary units. (B) Fluorescence time course, as in A, in the presence and absence of 250 nM Twf1 and a range of concentrations of CP. (C) Concentration-dependent effects of CP on the initial rate of decrease of actin filament fluorescence in the absence (black) and presence (green) of 250 nM Twf1. Rates were obtained from fluorescence curves in A and B. The theoretical curve (gray) was calculated, as described in the text, for direct inhibition of Twf1 by a range of CP concentrations. (D) TIRF microscopy of filaments incubated with Twf1 and CP. 1.5 μM monomeric actin (30% Alexa Fluor 488 labeled) was assembled into filaments in a flow cell, then 2 μM Twf1 with 3 μM CP in buffer pH 5.0 was applied at time zero, and filaments were monitored for 800 seconds. The time in seconds following addition of proteins is shown in the upper right corner of each panel. White arrows indicate the sites of the only two severing events observed in the field of view. (E) TIRF microscopy of filament growth after incubation with Twf1 and CP. Following incubation of filaments with Twf1 and CP in D, the immobilized filaments were incubated with fresh 1.5 μM actin monomers (30% Alexa Fluor 488 labeled) at time zero. Yellow arrowheads track the growth of barbed ends in consecutive frames. Blue arrows mark the original positions of barbed ends (at time zero) for frame of reference. The field in E is the same field as that shown in D. Movies of these TIRF microscopy experiments are provided in supplemental materials (Movie 4, supplementary material).

(Moon et al., 1993; Goode et al., 1998), filamentous actin structures that undergo rapid turnover. Cof1 plays an essential role in filament disassembly in vivo (Iida et al., 1993; Moon et al., 1993; Lappalainen and Drubin, 1997). This function has been demonstrated using the *cof1-22* allele, which has strong defects in filament disassembly in vitro and reduced rates of actin patch turnover in vivo (Lappalainen and Drubin, 1997; Lappalainen et al., 1997). To test whether Twf1 also promotes actin filament disassembly in vivo, we compared rates of patch turnover in wild-type, *twf1*Δ and *cof1-22* cells after treatment with Lat-A. Wild-type cells treated with 50 μM Lat-A for 5 minutes lost all actin filament structures detectable by staining with Alexa Fluor 568-congugated phalloidin (Fig. 10A,B). By contrast, *cof1-22* cells maintained visible actin patches after 5 minutes of treatment with Lat-A (Fig. 10A,B), consistent with previous reports (Lappalainen and Drubin, 1997; Lappalainen et al., 1997). *twf1*Δ cells also maintained visible actin staining, demonstrating a defect in actin turnover (Fig. 10A,B). The defects in *twf1*Δ cells were not as severe as those in *cof1-22* cells, evident by comparing the number of cells retaining visible F-actin structures (Fig. 10A) and the intensity of those structures (Fig. 10B). From these data, we conclude that Twf1 functions to promote actin filament disassembly in cells, consistent with its severing activity and with synthetic lethal interactions between *twf1*Δ and *cof1-22* mutations (Goode et al., 1998).

Discussion

We have described a new activity for the highly conserved actin-binding protein twinfilin. Until now, twinfilin has been thought to function solely as an actin-monomer-sequestering protein. Here, we have demonstrated that Twf1 also severs actin filaments to accelerate filament disassembly in vitro, and promotes rapid turnover of actin structures in vivo, consistent with this severing activity. Control experiments using the monomer-sequestering agent Lat-A differentiate between Twf1 functions in monomer sequestering versus filament binding and severing. Monomer sequestering by Twf1 (and

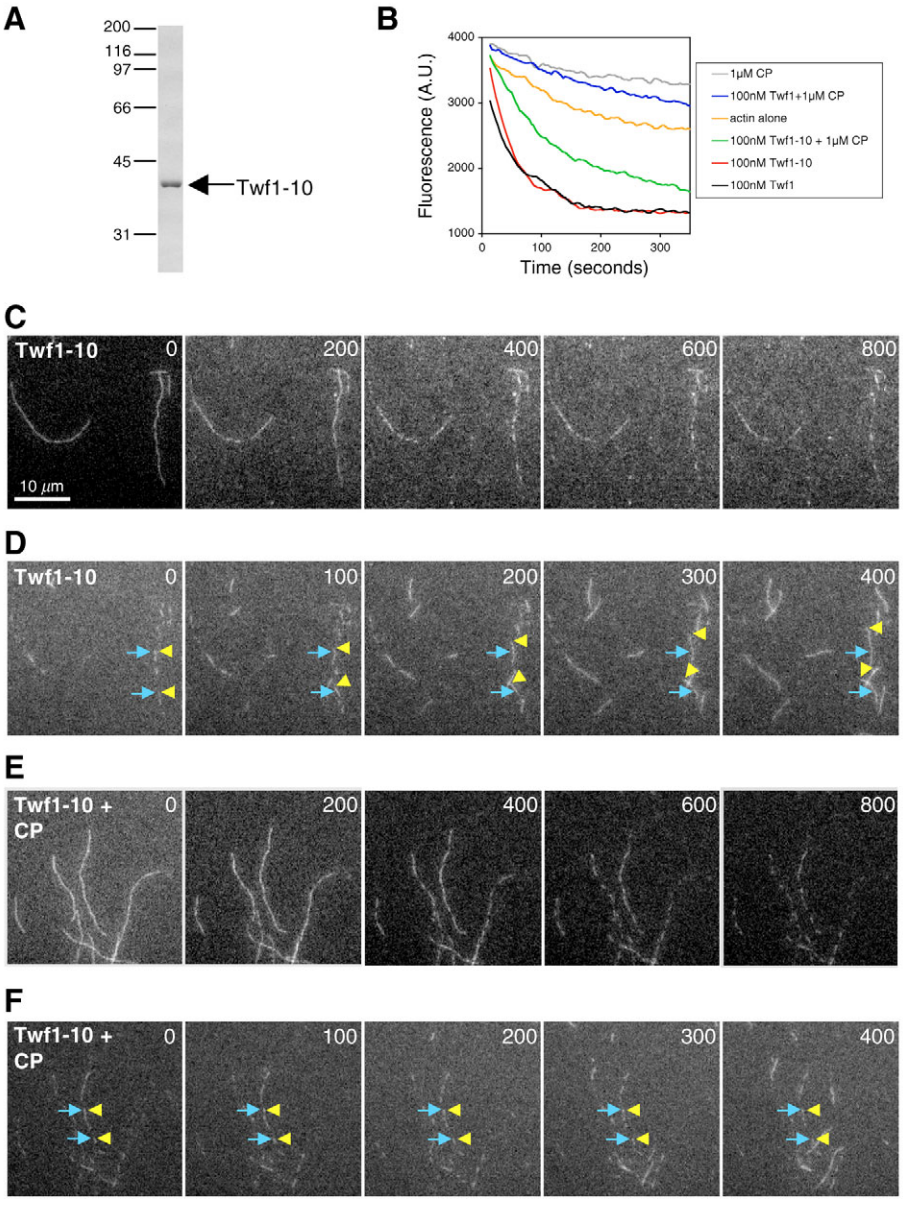

Fig. 7. CP inhibition of Twf1 filament binding and severing requires their direct interaction. (A) Coomassie-stained SDS-polyacrylamide gel of purified Twf1-10. Positions of molecular mass markers (kDa) are shown on the left. (B) Time course of actin filament fluorescence (30% pyrene labeled) after dilution at time zero (from 5 μM to 0.1 μM) in the presence of different concentrations of Twf1, Twf1-10 and/or CP at pH 5.0. A.U., arbitrary units. (C) TIRF microscopy of actin filaments incubated with Twf1-10. 1.5 μM monomeric actin (30% Alexa Fluor 488 labeled) was assembled into filaments in a flow cell, then 2 μM Twf1-10 in buffer pH 5.0 was applied at time zero. The time in seconds following addition of proteins is shown in the upper right corner of each panel. (D) Following filament severing by Twf1-10 in C, the immobilized filaments were incubated with fresh 1.5 μM actin monomers (30% Alexa Fluor 488 labeled) at time zero. Yellow arrowheads track the growth of barbed ends in consecutive frames. Blue arrows mark the original positions of barbed ends (at time zero) for frame of reference. The field in D is the same field as that shown in C. (E) TIRF microscopy of filaments incubated with both Twf1-10 and CP. Actin filaments were assembled as in C, then a mixture of 2 μM Twf1-10 and 3 μM CP in buffer pH 5.0 was applied at time zero. (F) Following filament severing in E, the immobilized filaments were incubated with fresh 1.5 μM actin monomers (30% Alexa Fluor 488 labeled) at time zero. Symbols are as in D. The field in F is the same field as that shown in E. Movies of these TIRF microscopy experiments are provided in supplemental materials (Movies 5 and 6, supplementary material).

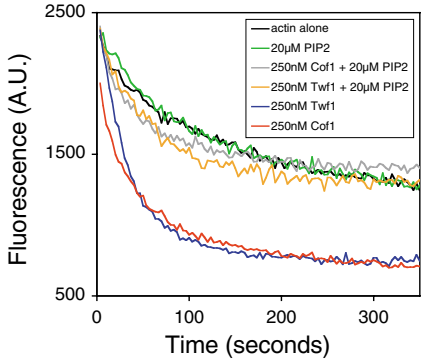

Fig. 8. PtdIns(4,5)P_2 inhibits Twf1 interactions with actin filaments. Time course of actin filament fluorescence (30% pyrene labeled) after dilution at time zero (from 5 μM to 0.1 μM) in the presence of the indicated concentrations of Twf1, Cof1 and/or PtdIns(4,5)P_2 (PIP2) at pH 5.0. A.U., arbitrary units.

Lat-A) at pH 7.5 induces slow net depolymerization of filaments, by binding to monomers as they dissociate from filament ends and blocking their re-addition onto filaments (Goode et al., 1998). Thus, monomer sequestering induces slow net disassembly of filaments, but does not affect rate of filament disassembly. By contrast, we have shown here that Twf1 at pH<6.0 dramatically increases rates of filament disassembly and visibly severs filaments; Lat-A does not have these effects. Thus, the pH-dependent function of Twf1 in filament severing and rapid depolymerization is distinct from its monomer-sequestering function. This severing activity might extend to twinfilins from other species and, if so, twinfilin would represent only the second identified family of widely conserved severing proteins, the other being ADF/cofilins (Bamburg, 1999). Importantly, twinfilin is distinct from ADF/cofilins in its regulation, being tightly controlled by pH and binding to capping protein.

Our data showing that Twf1 severs actin filaments also explain some previous observations. For example, *twf1*Δ yeast cells display enlarged cortical actin patches (Goode et al., 1998), and mutations in *Drosophila* twinfilin result in excessive F-actin structures in developing bristles (Wahlstrom et al., 2001). Such excess actin structures are consistent with defects in filament severing and disassembly. In addition, twinfilin mutations in both *S. cerevisiae* and *D. melanogaster* display synthetic defects with cofilin mutations. These observations have pointed to a possible function for twinfilin beyond monomer sequestration, consistent with our data here showing that twinfilin severs filaments in vitro and accelerates actin turnover in vivo. Thus, in addition to its well-established role as an actin-monomer-sequestering protein (Goode et al., 1998; Vartiainen et al., 2000; Wahlstrom et al., 2001; Vartiainen et

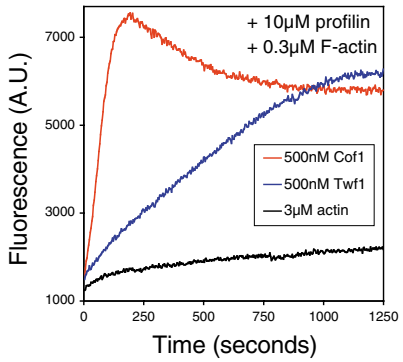

Fig. 9. Twf1 accelerates actin assembly seeded by pre-formed filaments. 3 μM monomeric actin (2% pyrene labeled) and 10 μM *S. cerevisiae* profilin were pre-mixed and added at time zero to 0.3 μM pre-formed actin filaments (F-actin) and 500 nM Cof1, 500 nM Twf1, or control buffer (3 μM actin) at pH 5.0. A.U., arbitrary units.

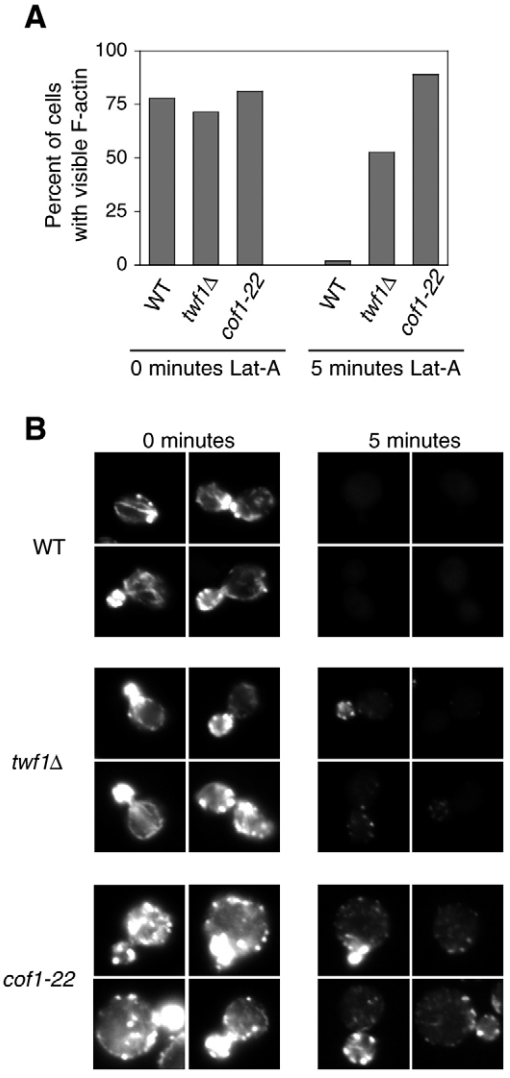

Fig. 10. Twf1 promotes actin filament disassembly in vivo. (A) Wild-type (WT), *twf1*Δ and *cof1-22* yeast cells were grown in parallel to OD_{600}=0.3, then treated with 50 μM Lat-A. Samples of cells were removed 0 and 5 minutes after addition of Lat-A, fixed in 5% formaldehyde, and stained for filamentous actin using Alexa Fluor 568-congugated phalloidin. Cells were visualized by fluorescence light microscopy and scored for the presence of visible actin patches and/or cables. >200 cells were counted for each data point, and similar results were obtained in two independent experiments. Treatment of cells with control buffer caused no loss of actin structures (not shown). (B) Representative wild-type (WT), *twf1*Δ and *cof1-22* cells stained with Alexa Fluor 568-congugated phalloidin 0 minutes and 5 minutes after treatment with Lat-A.

al., 2003), twinfilin also interacts with filaments and directly promotes filament turnover.

Two lines of evidence demonstrate the physiological relevance of the activities we have characterized for yeast twinfilin (Twf1). First, Twf1 promotes the rapid turnover of filamentous actin structures (patches) in yeast cells grown under standard conditions. Second, the severing activity of Twf1 is regulated by direct interactions with CP, a key in vivo ligand of Twf1 (Palmgren et al., 2001; Falck et al., 2004). Why then does Twf1 not sever filaments at a more neutral pH in vitro? One possibility is that local variations and/or fluctuating pH levels in yeast cytosol and/or subcompartments provide environments with pH<6.0. A second possibility is that cellular Twf1 severs filaments at more neutral pH following post-translational modification (of either Twf1 or actin) and/or interactions with specific ligands, which can alter the pH dependence of its activity. Thus, it will also be important to investigate post-translational modifications of twinfilin. Many cofilin isoforms are regulated by phosphorylation at Ser3 (Bamburg, 1999), and sequence alignments between cofilin and twinfilin show that the two ADFH domains in yeast Twf1 possess serine residues at the second and fifth positions (Ser2, Ser5, Ser167 and Ser170) (Goode et al., 1998). This raises the possibility of Twf1 phosphoregulation at similar sites to cofilin. These and/or other modifications might alter Twf1 activities to promote filament binding and severing at a more neutral pH.

To understand better the Twf1 severing mechanism, it will be important to define the Twf1 surfaces that mediate actin filament binding. In particular, the two ADFH domains, each of which shows affinity for actin monomers (Ojala et al., 2002), might play distinct roles in severing. The C-terminal ADFH domain of mouse twinfilin binds to actin monomers with higher affinity than the N-terminal ADFH domain, and with similar affinity to full-length twinfilin (Ojala et al., 2002). Thus, the C-terminal ADFH domain might function primarily in monomer binding, whereas the N-terminal ADFH domain could mediate filament severing, as it is dispensable for efficient monomer binding.

Our demonstration that yeast capping protein (CP) inhibits Twf1 severing is the first function ascribed to this cellular interaction. Importantly, we found that inhibition is abolished by Twf1-10, a mutant that disrupts binding to CP (Falck et al., 2004). Since Twf1 and CP levels are similar in yeast cells (Palmgren et al., 2001; Kim et al., 2004; our unpublished data), CP has the capacity in principle to regulate most of the cellular Twf1. Importantly, *twf1-10* disrupts localization of Twf1 to actin patches (like *cap2*Δ mutations) and is synthetic lethal with *cof1-22* and *pfy1-4*, suggesting a loss of *TWF1* function (Palmgren et al., 2002; Falck et al., 2004). Our results alone might predict instead that *twf1-10* should cause hyper-severing of filaments (since its activity would be uninhibited by CP). However, CP binding appears to regulate Twf1 function on multiple levels in vivo, including Twf1 localization to patches, inhibition of filament severing, and possibly Twf1 monomer sequestering by an unknown mechanism. Thus, open questions to address include: what regulates the CP-Twf1 interaction, and how is the control of Twf1 severing of filaments coordinated with Twf1 sequestering of monomers?

In summary, the regulation of Twf1-induced filament severing in vivo might be subject to control by multiple mechanisms, including local pH, post-translational modifications, CP interactions, phospholipid binding, and possibly actin monomer levels. These integrated signals probably maintain a balance between filament severing and monomer sequestration in vivo, and open new possibilities for the role of twinfilin and other cellular factors in the control of actin dynamics.

Materials and Methods

Protein expression and purification

Full-length *S. cerevisiae* wild-type twinfilin (Twf1) and mutant Twf1-10 proteins were expressed and purified as previously described (Goode et al., 1998) with minor modifications. Briefly, the *TWF1* coding region was amplified from *S. cerevisiae* genomic DNA by PCR using oligonucleotides that introduce *Xho*I and *Hin*dIII sites at the 5′ and 3′ ends of the fragment, respectively. This fragment was subcloned into the *Xho*I and *Hin*dIII sites of the pGAT2 plasmid (Peranen et al., 1996). The Twf1-10 bacterial expression plasmid (Falck et al., 2004) was a kind gift from P. Lappalainen (Institute of Biotechnology, University of Helsinki, Helsinki, Finland). Twf1 and Twf1-10 were expressed as glutathione-*S*-transferase (GST) fusion proteins in *Escherichia coli* strain BL21(DE3). Cells were grown to log phase at 37°C, and then expression was induced by addition of 0.4 mM isopropyl-β-D-thiogalactopyranoside (IPTG). Cells were grown for an additional 4 hours at 37°C, harvested by centrifugation, washed with 30 ml PBS (40 mM sodium phosphate buffer pH 7.4, 300 mM NaCl), and resuspended in 15 ml PBS supplemented freshly with 0.5 mM dithiothreitol (DTT) and 1 mM phenylmethylsulphonyl fluoride (PMSF). Cells were lysed by incubation with lysozyme (0.5 mg/ml) on ice for 15 minutes followed by sonication. The cell lysate was clarified by centrifugation at 14,000 ***g*** for 15 minutes and incubated at 4°C (rotating) for 2 hours with 0.5 ml glutathione-agarose beads (Sigma). Beads were washed 5 times in PBS, then twinfilin was cleaved from GST by incubation overnight at 4°C with thrombin (5 U/ml; Sigma). Beads were pelleted, and the supernatant was concentrated to ~0.3 ml in a Microcon-10 device (Millipore), then further purified by size exclusion chromatography on a Superose12 column (Amersham Biosciences) equilibrated in TN buffer (10 mM Tris-HCl pH 7.5, 50 mM NaCl, 0.5 mM DTT). Peak fractions were pooled, concentrated in a Microcon-10 device, aliquoted, snap-frozen in N_2, and stored at –80°C.

Rabbit skeletal muscle actin was purified (Spudich and Watt, 1971) and labeled on Cys374 with pyrenyliodoacetamide (Pollard and Cooper, 1984; Higgs et al., 1999) or on lysines (Kellogg et al., 1988) with Alexa Fluor 488 carboxylic acid succinimidyl ester. *S. cerevisiae* actin was purified (Goode, 2002) and labeled on Cys374 with pyrenyliodoacetamide (Pollard and Cooper, 1984; Higgs et al., 1999) as described. *S. cerevisiae* cofilin (Lappalainen et al., 1997), capping protein (Amatruda and Cooper, 1992) and profilin (Wolven et al., 2000) were purified as described. Human plasma gelsolin was purchased from Cytoskeleton, and PtdIns(4,5)P_2 was purchased from EMD Biosciences.

Actin filament depolymerization kinetics

For pyrene-fluorescence-monitored actin filament disassembly assays, 5 μM gel-filtered rabbit muscle actin (30% pyrene labeled) was polymerized at 25°C for 1 hour in F-buffer (10 mM Tris-HCl pH 7.5, 0.2 mM DTT, 0.2 mM $CaCl_2$, 50 mM KCl, 2 mM $MgCl_2$, and 0.7 mM ATP). Prior to each reaction, 10 μl TN buffer or proteins in TN buffer were mixed with 88 μl F-buffer made with MES substituted for Tris-HCl and adjusted to the experimental pH. All pyrene-labeled actin filament disassembly assays (Figs 1 and 2, and data not shown) were duplicated using MES-buffered and Tris-buffered solutions. In all cases, buffer pH was determined in the final reaction solution, and results from reactions in MES-buffered solutions were indistinguishable from results from reactions in solutions buffered with Tris-HCl. Data in Figs 1, 2, 7 and 8 were obtained in MES F-buffer, and data in Figs 5 and 6 were obtained in Tris-HCl F-buffer. To initiate filament disassembly, the 98 μl mixture (above) was added to 2 μl pre-assembled actin filaments (final concentration 0.1 μM rabbit muscle actin in reaction). Pre-cut pipet tips were used for all manipulations of actin filaments, and care was taken to avoid filament shearing. Pyrene fluorescence was monitored at 25°C over time at an excitation of 365 nm and emission of 407 nm in a fluorescence spectrophotometer (Photon Technology International). Depolymerization rates were determined by measuring the initial slope of fluorescence curves within the first 200 seconds of reactions. For depolymerization of gelsolin-capped actin filaments (Fig. 5), 5 μM gel-filtered rabbit muscle actin (40% pyrene labeled) was polymerized in the presence of 25 nM human plasma gelsolin. Depolymerization of gelsolin-capped filaments was induced by dilution and monitored by pyrene fluorescence as above. For depolymerization reactions monitored by light scattering, the following modifications were made. Actin filaments were polymerized at 5 μM from unlabeled rabbit muscle actin. Pre-assembled actin filaments were diluted from 5 μM to 0.25 μM in 100 μl reactions, and monitored by excitation and emission at 400 nm.

Fluorescence microscopy of actin filaments

For the experiments in Fig. 3C and Fig. S1 (supplementary material), pyrene-

fluorescence-monitored actin filament disassembly assays were performed as above. For each reaction, 10 μl aliquots were removed at the indicated time points (5, 50, 100 and 600 seconds) and incubated with 0.3 μM Alexa Fluor 488-conjugated phalloidin for 5 minutes at room temperature. The time required for reaction setup and aliquot removal was 5 seconds, representing the earliest visualized time point for each reaction. Aliquots were subsequently diluted fivefold with F-buffer (pH 5) containing 0.5% methylcellulose, and 1 μl was applied to a nitrocellulose-coated coverslip (made by applying a 0.1% solution of nitrocellulose in amylacetate). Actin filaments were examined by fluorescence microscopy using a Zeiss Axioskop-2 mot *plus* microscope (Carl Zeiss) equipped with a Hamamatsu C4742-95 CCD camera (Orca-ER; Hamamatsu Photonics) camera running OpenLab software (Improvision).

Actin filament assembly assays

Gel-filtered Ca^{2+}-ATP rabbit skeletal muscle actin monomers (5% pyrene labeled) were prepared as described (Moseley and Goode, 2005). Ca^{2+}-ATP actin was converted to Mg^{2+}-ATP actin monomers immediately prior to initiation of a reaction, and actin assembly was monitored as previously described (Moseley and Goode, 2005).

Total internal reflection fluorescence (TIRF) microscopy

TIRF microscopy was performed as described (Kovar et al., 2003; Kovar and Pollard, 2004) with minor modifications. Glass flow cells were washed extensively with 1% BSA and equilibrated with TIRF buffer (10 mM imidazole pH 7.0, 50 mM KCl, 1 mM $MgCl_2$, 1 mM EGTA, 50 mM DTT, 0.2 mM ATP, 50 μM $CaCl_2$, 15 mM glucose, 20 μg/ml catalase, 100 μg/ml glucose oxidase, 0.5% methylcellulose of 4000 centipoise). Mixtures of unlabeled actin and Alexa Fluor 488-labeled monomers (final actin concentration 1.5 μM, 30% labeled) were mixed with TIRF buffer, transferred to a flow cell, and polymerized for approximately 5 minutes to the lengths observed at the beginning frames in Fig. 4A-C. Samples of 2 μM Twf1, 2 μM Twf1-10, 2 μM Twf1 with 3 μM CP, 2 μM Twf1-10 with 3 μM CP, 10 μM latrunculin-A (lat-A), or control buffer were prepared in TIRF buffer adjusted to the appropriate pH, and added to flow cells in the absence of actin monomers. At pH 5.0, actin filaments nonspecifically adhere to the slides for unknown reasons. However, this immobility permits observation of filaments in a single focal field for long periods of time. To flow fresh actin monomers into chambers with immobilized, severed filaments (Fig. 4C, Fig. 6D, Fig. 7C,E), mixtures of unlabeled and Alexa-green-labeled actin monomers were mixed as above in TIRF buffer (pH 7.5) and flowed into chambers using wicks to facilitate exchange of solutions. Images were collected continuously, throughout addition/exchange of buffers and proteins, using a Hamamatsu C4742-95 CCD camera (Orca-ER) on an Olympus IX-70 microscope. Images acquired at 20-second intervals were processed with IMAGEJ software (http://rsb.info.nih.gov/ij) as described (Amann and Pollard, 2001; Kovar et al., 2003).

Measurement of actin patch turnover in yeast cells

Isogenic wild-type, *twf1*Δ and *cof1-22* yeast strains (Lappalainen and Drubin, 1997; Lappalainen et al., 1997; Goode et al., 1998) were grown in 10 ml YPD cultures at 25°C to log phase (OD_{600}~0.3) (Guthrie and Fink, 1991). Cells were then concentrated by centrifugation, resuspended in 600 μl YPD, and grown an additional 30 minutes at 25°C. Cells were then treated with 50 μM lat-A (generously provided by Phil Crews, University of California, Santa Cruz, CA) or control buffer, and mixed by vortexing. 100 μl samples of cells were removed at time points of 0 and 5 minutes, fixed in formaldehyde (5% final concentration), stained with Alexa Fluor 568-conjugated phalloidin (Invitrogen) as described (Pringle et al., 1991), and examined by fluorescence microscopy using a Zeiss Axioskop-2 microscope equipped with a Hamamatsu C4742-95 CCD camera (Orca-ER) camera running OpenLab software. The number of cells with visible actin patches or cables was measured at each time point for each strain (>200 cells). Similar results were obtained in two independent experiments. Two different wild-type strains (isogenic for *cof1-22* and *twf1*Δ alleles, respectively) gave identical results; data for one is presented in Fig. 10. Treatment of cells with control buffer caused no detectable disassembly of actin structures (not shown).

We thank R. Mahaffy for providing Alexa-labeled actin and P. Lappalainen for helpful discussions. H.I.B. was supported by a predoctoral fellowship from the American Heart Association, D.R.K. by a postdoctoral fellowship from the NIH, T.D.P. by the NIH (GM26338), and B.L.G. by the NIH (GM63691) and American Cancer Society (RSG-04-176-CSM).

References

Amann, K. J. and Pollard, T. D. (2001). Direct real-time observation of actin filament branching mediated by Arp2/3 complex using total internal reflection fluorescence microscopy. *Proc. Natl. Acad. Sci. USA* **98**, 15009-15013.

Amatruda, J. F. and Cooper, J. A. (1992). Purification, characterization, and immunofluorescence localization of *Saccharomyces cerevisiae* capping protein. *J. Cell Biol.* **117**, 1067-1076.

Bamburg, J. R. (1999). Proteins of the ADF/cofilin family: essential regulators of actin dynamics. *Annu. Rev. Cell Dev. Biol.* **15**, 185-230.

Blanchoin, L. and Pollard, T. D. (1999). Mechanism of interaction of Acanthamoeba actophorin (ADF/Cofilin) with actin filaments. *J. Biol. Chem.* **274**, 15538-15546.

Carlier, M. F., Laurent, V., Santolini, J., Melki, R., Didry, D., Xia, G.-X., Hong, Y., Chua, N.-H. and Pantaloni, D. (1997). Actin depolymerizing factor (ADF/cofilin) enhances the rate of filament turnover: Implication in actin-based motility. *J. Cell Biol.* **136**, 1307-1323.

Carlier, M. F., Ressad, F. and Pantaloni, D. (1999). Control of actin dynamics in cell motility. Role of ADF/cofilin. *J. Biol. Chem.* **274**, 33827-33830.

Du, J. and Frieden, C. (1998). Kinetic studies on the effect of yeast cofilin on yeast actin polymerization. *Biochemistry* **37**, 13276-13284.

Falck, S., Paavilainen, V. O., Wear, M. A., Grossmann, J. G., Cooper, J. A. and Lappalainen, P. (2004). Biological role and structural mechanism of twinfilin-capping protein interaction. *EMBO J.* **23**, 3010-3019.

Goode, B. L. (2002). Purification of yeast actin and actin-associated proteins. *Meth. Enzymol.* **351**, 433-441.

Goode, B. L., Drubin, D. G. and Lappalainen, P. (1998). Regulation of the cortical actin cytoskeleton in budding yeast by twinfilin, a ubiquitous actin monomer-sequestering protein. *J. Cell Biol.* **142**, 723-733.

Guthrie, C. and Fink, G. R. (1991). Guide to yeast genetics and molecular biology. *Meth. Enzymol.* **194**, 182-187.

Higgs, H. N., Blanchoin, L. and Pollard, T. D. (1999). Influence of the C terminus of Wiskott-Aldrich syndrome protein (WASp) and the Arp2/3 complex on actin polymerization. *Biochemistry* **38**, 15212-15222.

Iida, K., Moriyama, K., Matsumoto, S., Kawasaki, H., Nishida, E. and Yahara, I. (1993). Isolation of a yeast essential gene, *COF1*, that encodes a homologue of mammalian cofilin, a low-Mr actin-binding and depolymerizing protein. *Gene* **124**, 115-120.

Kellogg, D. R., Mitchison, T. J. and Alberts, B. M. (1988). Behaviour of microtubules and actin filaments in living Drosophila embryos. *Development* **103**, 675-686.

Kim, K., Yamashita, A., Wear, M., Maeda, Y. and Cooper, J. A. (2004). Capping protein binding to actin in yeast: biochemical mechanism and physiological relevance. *J. Cell Biol.* **164**, 567-580.

Kovar, D. R. and Pollard, T. D. (2004). Insertional assembly of actin filament barbed ends in association with formins produces piconewton forces. *Proc. Natl. Acad. Sci. USA* **101**, 14725-14730.

Kovar, D. R., Kuhn, J. R., Tichy, A. L. and Pollard, T. D. (2003). The fission yeast cytokinesis formin Cdc12p is a barbed end actin filament capping protein gated by profilin. *J. Cell Biol.* **161**, 875-887.

Kovar, D. R., Wu, J. Q. and Pollard, T. D. (2005). Profilin-mediated competition between capping protein and formin Cdc12p during cytokinesis in fission yeast. *Mol. Biol. Cell* **16**, 2213-2224.

Kuhn, J. R. and Pollard, T. D. (2005). Real-time measurements of actin filament polymerization by total internal reflection fluorescence microscopy. *Biophys. J.* **88**, 1387-1402.

Lappalainen, P. and Drubin, D. G. (1997). Cofilin promotes rapid actin filament turnover *in vivo*. *Nature* **388**, 78-82.

Lappalainen, P., Federov, E. V., Federov, A. A., Almo, S. C. and Drubin, D. G. (1997). Essential functions and actin-binding surfaces of yeast cofilin revealed by systematic mutagenesis. *EMBO J.* **16**, 5520-5530.

Lappalainen, P., Kessels, M. M., Cope, M. J. and Drubin, D. G. (1998). The ADF homology (ADF-H) domain: a highly exploited actin-binding module. *Mol. Biol. Cell* **9**, 1951-1959.

Moon, A. L., Janmey, P. A., Louie, K. A. and Drubin, D. G. (1993). Cofilin is an essential component of the yeast cortical cytoskeleton. *J. Cell Biol.* **120**, 421-435.

Moseley, J. B. and Goode, B. L. (2005). Differential activities and regulation of *S. cerevisiae* formins Bni1 and Bnr1 by Bud6. *J. Biol. Chem.* **280**, 28023-28033.

Ojala, P. J., Paavilainen, V. O., Vartiainen, M. K., Tuma, R., Weeds, A. G. and Lappalainen, P. (2002). The two ADF-H domains of twinfilin play functionally distinct roles in interactions with actin monomers. *Mol. Biol. Cell* **13**, 3811-3821.

Paavilainen, V. O., Merckel, M. C., Falck, S., Ojala, P. J., Pohl, E., Wilmanns, M. and Lappalainen, P. (2002). Structural conservation between the actin monomer-binding sites of twinfilin and actin-depolymerizing factor (ADF)/cofilin. *J. Biol. Chem.* **277**, 43089-43095.

Palmgren, S., Ojala, P. J., Wear, M. A., Cooper, J. A. and Lappalainen, P. (2001). Interactions with PIP2, ADP-actin monomers, and capping protein regulate the activity and localization of yeast twinfilin. *J. Cell Biol.* **155**, 251-260.

Palmgren, S., Vartiainen, M. and Lappalainen, P. (2002). Twinfilin, a molecular mailman for actin monomers. *J. Cell Sci.* **115**, 881-886.

Peranen, J., Rikkonen, M., Hyvonen, M. and Kääriäinenen, L. (1996). T7 vectors with a modified T7lac promoter for expression of proteins in *Escherichia coli*. *Anal. Biochem.* **236**, 371-373.

Pollard, T. D. and Cooper, J. A. (1984). Quantitative analysis of the effect of *Acanthamoeba* profilin on actin filament nucleation and elongation. *Biochemistry* **23**, 6631-6641.

Pringle, J. R., Adams, A. E. M., Drubin, D. G. and Haarer, B. K. (1991). Immunofluorescence methods for yeast. In *Guide to Yeast Genetics and Molecular Biology*, *Vol. 194* (ed. C. Guthrie and G. R. Fink), pp. 565-601. San Diego: Academic Press.

Spudich, J. A. and Watt, S. (1971). The regulation of rabbit skeletal muscle contraction. I. Biochemical studies of the interaction of the tropomyosin-troponin complex with actin and the proteolytic fragments of myosin. *J. Biol. Chem.* **246**, 4866-4871.

Theriot, J. A. (1997). Accelerating on a treadmill: ADF/cofilin promotes rapid actin filament turnover in the dynamic cytoskeleton. *J. Cell Biol.* **136**, 1165-1168.

Vartiainen, M., Ojala, P. J., Auvinen, P., Peranen, J. and Lappalainen, P. (2000). Mouse A6/twinfilin is an actin monomer-binding protein that localizes to the regions of rapid actin dynamics. *Mol. Cell. Biol.* **20**, 1772-1783.

Vartiainen, M. K., Sarkkinen, E. M., Matilainen, T., Salminen, M. and Lappalainen, P. (2003). Mammals have two twinfilin isoforms whose subcellular localizations and tissue distributions are differentially regulated. *J. Biol. Chem.* **278**, 34347-34355.

Wahlstrom, G., Vartiainen, M., Yamamoto, L., Mattila, P. K., Lappalainen, P. and Heino, T. I. (2001). Twinfilin is required for actin-dependent developmental processes in *Drosophila*. *J. Cell Biol.* **155**, 787-796.

Wolven, A. K., Belmont, L. D., Mahoney, N. M., Almo, S. C. and Drubin, D. G. (2000). In vivo importance of actin nucleotide exchange catalyzed by profilin. *J. Cell Biol.* **150**, 895-904.